

# Particle Production in $\sqrt{s_{\text{NN}}} = 2.76$ TeV Heavy Ion Collisions

Johann Rafelski<sup>1</sup> and Jean Letessier<sup>1,2</sup>

<sup>1</sup>*Department of Physics, University of Arizona, Tucson, Arizona 85721, USA and*

<sup>2</sup>*LPTHE, Université Paris 6 et 7, Paris 75005, France*

(Dated: December 7, 2010)

We consider, within the statistical hadronization model, the near central rapidity  $y \simeq 0$  integrated hadron yields expected at LHC  $\sqrt{s_{\text{NN}}} = 2.76$  TeV ion reactions, for which the total charged hadron rapidity most central head-on collision yield is  $dh/dy|_{y=0} \simeq 1800$ . For the chemical equilibrium SHM, we discuss composition of  $dh/dy$  as function of hadronization temperature. For chemical non-equilibrium SHM, we input the specific strangeness yield  $s/S$ , demand explosive disintegration and study the break up as a function of the critical hadronization pressure  $P$ . We develop observables distinguishing the hadronization models and conditions.

PACS numbers: 12.38.Mh, 24.10.Pa, 25.75.-q

**Introduction:** According to the theory of strong interactions, Quantum Chromo-Dynamics (QCD), quarks and gluons are confined inside hadrons. At sufficiently high temperature lattice computations demonstrate that the deconfined Quark–Gluon Plasma (QGP) prevails [1]. We seek to prove this QCD paradigm in high energy heavy ion collisions where heavy nuclei are crushed on each other, forming a small drop of thermalized deconfined QGP matter. This drop hadronizes into a high multiplicity of particles and we seek to determine the physical properties of QGP considering this multiparticle final state.

At LHC energy  $\sqrt{s_{\text{NN}}} = 2.76$  TeV, for near head-on 5% most central Pb–Pb collisions, the pseudo-rapidity density of primary charged particles at mid-rapidity is  $dh/d\eta = 1584 \pm 4 \pm 76$  *syst*, an increase of about a factor 2.2 to central Au–Au RHIC collisions at  $\sqrt{s_{\text{NN}}} = 0.2$  TeV [2]. The study of particle yields per unit of rapidity obtained after integration of transverse momentum particle spectra eliminates the need to model the distortion of spectra introduced by explosive dynamics (see, e.g., [3]) of highly compressed matter created in high energetic collisions.

Following the reference [3], where deformation of the spectra were studied in model cases, we interpret the measured  $dh/d\eta$  to be equivalent to a central rapidity density  $dh/dy \simeq 1800$ . This experimental result enables us to offer prediction for a variety of different particle multiplicities, dependent on adopted hadronization model and a first interpretation in terms of particle source bulk properties.

**SHM — Statistical hadronization model:** QGP hadronic particle production yields are generally considered within the statistical hadronization model (SHM) [4, 5]. SHM has been successful in describing hadron production in heavy ion collisions for different colliding systems and energies. Some view the SHM as a qualitative model and as such one is tempted to seek *simplicity* in an effort to obtain an estimate of the yields for all hadrons with just a small number of parameters [6–8].

Improving experimental precision, along with physics motivation based in qualitative dynamics of the

hadronization process has stimulated refinements involving a greater parameter set allowing to control the dynamically established yield of different quark flavors, generally referred to as chemical non-equilibrium SHM [5]. This is achieved by introducing statistical occupancy parameters  $\gamma_i > 1$ ,  $i = q, s, c$ , where  $s$  is the strange and  $c$  the charm quark flavor. It can be assumed that up and down quark yields  $q = u, d$  are equally equilibrated. We will not discuss the charm flavor here.

Moreover, we are interested in precise description of the bulk properties of the particle source, such as size, energy and entropy content of the QGP fireball. This requires precise capability to extrapolate observed hadron yields to unobserved kinematic domains and unobserved particle types. This is the case for chemical non-equilibrium approach as demonstrated by the smooth systematic behavior of physical observables as a function of collision conditions such as reaction energy [5] or collision centrality [9].

With increasing collision energy, the baryon content at central rapidity decreases rapidly. It is expected that there remains a small excess of matter over antimatter at central rapidity at LHC [10]. In SHM, this is governed by chemical parameters  $\lambda_q, \lambda_s$  (equivalent to  $\mu_B, \mu_S$ , the baryon and strangeness chemical potentials of matter). Determination of values of  $\mu_B, \mu_S$  must await additional experimental data. We present, for orientation of how the baryon–antibaryon yields vary, results testing different values of the expected potentials choosing a fixed input value  $\lambda_q = 1.0055$ , which results for in  $\mu_B \simeq 2.9 \pm 0.3$  MeV,  $\mu_S \simeq 0.7 \pm 0.3$  MeV, and  $\mu_B \simeq 2.0 \pm 0.2$  MeV,  $\mu_S \simeq 0.45 \pm 0.05$  MeV in case of equilibrium and non-equilibrium models, respectively.

Note that since the number of strange and antistrange quarks in hadrons has to be equal,  $\lambda_s$ , and thus  $\mu_S$  is determined in order to satisfy this constraint. Another constraint is also implemented, the total charge per baryon has to be  $Q/B = 0.4$ , since the stopping of electrically charged matter (protons) within a rapidity interval is the same as that of all baryonic matter (protons and neutrons). This is achieved by a suitable tiny up-down quark asymmetry, a feature implemented in the SHARE suit of

programs we are using [4].

In the usual procedure of statistical hadronization modeling, the particle yields are used to find best statistical parameters. The SHARE suit of programs was written in a more flexible way to allow also mixed a fit, that is a fit where a few particle yields can be combined with the given ‘measured’ statistical parameters to obtain best fit of other statistical parameters. When we were developing SHARE, this feature was created since a parameter such as temperature could be measured using spectral shape and thus should be not fitted again in the yield description but be used as an experimental input. To be general, this feature was extended to all statistical parameters of the SHARE program.

This feature allows us to perform a fit of the mix of statistical parameters and particle yields. Our procedure has been outlined before [15] and is, here, applied for the first time including LHC experimental data. This allows us to predict within the chemical equilibrium and non-equilibrium SHM models the differing pattern of particle production such that  $dh/dy$  is fixed.

**Importance of understanding chemical (non)-equilibrium:** When chemical non-equilibrium is derived from the particle yields, generating in the fit to data  $\gamma_i \neq 1$ , this suggests a dynamical picture of an explosively expanding and potentially equilibrated QGP, decaying rapidly into free streaming hadrons. Without a significant re-equilibration, the (nearly) equilibrated QGP cannot produce chemically equilibrated hadron yield. The high intrinsic QGP entropy content explains why equilibrated QGP turns into chemically overpopulated (oversaturated) HG phase space. — The fast breakup of QGP means that the emerging hadrons do not have opportunity to re-establish chemical equilibrium in the HG phase.

The differentiation of chemical equilibrium and non-equilibrium SHM models will be one of the challenges we address in our present discussion facing the SHM model and interpretation of the hadron production. One could think that resolution of this matter requires a good fit of SHM parameters to the data. However, with the large errors on particle yields and lack of sensitivity to  $\gamma_q$ , this is not easy.

The light quark phase space occupancy parameter  $\gamma_q$  can be only measurable by determining overall baryon to meson yield, and this cannot be done without prior measurement of hadronization temperature  $T$ . When particle yield data is not available to measure both  $T$  and  $\gamma_q$ , one can fit only  $\gamma_s/\gamma_q$  to the data, which is then reported as  $\gamma_s$  accompanied by the tacit assumption  $\gamma_q = 1$ . Since  $\gamma_s$  (or  $\gamma_s/\gamma_q$ ) controls the overall (relative) yield of strange quarks, one expects and finds in most environments  $\gamma_s \neq 1$  (or  $\gamma_s/\gamma_q \neq 1$ ) and a value which increases with system size, and often with energy.

We recognize considerable physics implication of understanding the value of  $\gamma_q$ , as this relates directly to the measurement of  $T$ , related to the phase transformation condition  $T_{tr}$  of QGP to hadrons, studied within lattice QCD. In the chemical equilibrium context,  $T \simeq T_{tr}$ .

On the other hand, the chemical non-equilibrium SHM implies rapid expansion and supercooled transformation and hence  $T < T_{tr}$ , with estimated difference at 10–15 MeV [14].

For lower heavy ion reaction energies as compared to LHC, one can also determine the baryochemical potential at hadronization. This then allows to compare lattice QCD transformation condition,  $T_{tr}$ ,  $\mu_{B,tr}$  [11, 12], with the data fit in the chemical equilibrium SHM [10, 13] and chemical non-equilibrium SHM [5]. One finds that lattice results are much flatter compared to the equilibrium SHM, that is  $T_{tr}$  drops off much slower with  $\mu_{B,tr}$ . On the other hand, the non-equilibrium SHM parallels the lattice data 15 MeV below the transformation boundary. This favors, on theoretical grounds, the chemical non-equilibrium approach.

**LHC predictions assuming chemical equilibrium:** Just one observable, the number of charged particles  $dh/dy \simeq 1800$ , fixes within statistical model a large number of particle yields. This is allowing to test SHM model. We explore chemical equilibrium and non-equilibrium conditions in turn. We will show that many of the particle yields vary little as function of hadronization condition for a prescribed  $dh/dy$ . We present an unusual number of digits, a precision which has nothing to do with experiment but is needed to facilitate reproducibility of our results. We further state the propagation error of the error  $\Delta dh/dy = 100$  which is mostly confined to the volume, but is in some cases also visible in  $T$  and also further below in the chemical non-equilibrium parameters  $\gamma_q$ ,  $\gamma_s$ ,

Our procedure for the equilibrium SHM is as follows: in the chemical equilibrium model, see table I, we set  $\gamma_q = 1$ ,  $\gamma_s = 1$  and as noted also on other grounds  $\lambda_q = 1.0055$ .  $\lambda_s$  follows from the constraint of strangeness balance  $s - \bar{s} = 0$ . All our results maintain a fixed  $Q/B = 0.4$ . We then see that, at fixed hadronization temperature  $T$  chosen in table I to be 159, 169, 179, 189 MeV, the yield of charged hadrons  $dh/dy$  is, correlated to the source volume  $dV/dy$ . Volume varies strongly with temperature, since particle yields scale, for  $T \gg m$ , as  $VT^3$ . Actually, since  $T \gg m$  condition is not satisfied, the volume is changing more rapidly so that  $T^k dV/dy = \text{Const.}$ ,  $k \simeq 7.2$ .

Since charged particle number is fixed, we also expect that entropy of the bulk is fixed and that is true; up to a small variation due to variation with  $T$  in relative yield of heavy hadrons, the entropy content is  $dS/dy = 14800 \pm 400$ . As temperature increases, the proportion of heavy mass charged particles increases, and thus the pion yield and even the kaon yield slightly decrease with increasing  $T$ . Baryon yields is most sensitive to  $T$ :  $\Omega$  doubles in yield in the temperature interval considered. Our choice of  $\lambda_q$  fixes for each hadronization temperature the per rapidity net baryon yield also shown in table I. — We believe our choice is reasonable and has been made also so that we see that there is no need to distinguish particles from antiparticles.

TABLE I: Chemical equilibrium particle yields at  $\sqrt{s_{NN}} = 2.76$  TeV. Top section: input properties; middle section: properties of the fireball associated with central rapidity; bottom section: expected particle yields, and some select ratios.

\* signals an input value, and \*\* a result directly following from input value (combined often with a constraint). All yields, but  $\pi_{WD}^0$ , without weak decay feed to particle yields. Error in  $dV/dy$  corresponds to error in  $dh/dy$  equal 100.

$T^*$ [MeV]	159	169	179	189
$\gamma_q^*$	1	1	1	1
$\gamma_s^*$	1	1	1	1
$\lambda_q^*$	1.0055	1.0055	1.0055	1.0055
$10^3(\lambda_s - 1)^{**}$	2.06	1.45	0.89	0.39
$(Q/B)^*$	0.4000	0.4000	0.4000	0.4000
$(s - \bar{s})^*$	0.0000	0.0000	0.0000	0.0000
$(dh/dy)^*$	1800	1800	1800	1800
$dV/dy$ [fm <sup>3</sup> ]	5285±147	3452±96	2286±64	1538±43
$dS/dy$	15155	14940	14690	14420
$s/S$	0.0245	0.0255	0.0263	0.0270
$P$ [MeV/fm <sup>3</sup> ]	64.1	100	153	231
$E/Ts$	0.859	0.86	0.87	0.87
$P/E$	0.164	0.158	0.153	0.150
$E/V$ [GeV/fm <sup>3</sup> ]	0.392	0.632	0.997	1.54
$\pi^-, \pi^+$	839	830	821	813
$K^-$	141.3	140.8	139.0	136.8
$K^+$	142.1	141.6	140.1	137.8
$p$	53.6	63.1	72.0	79.8
$\bar{p}$	51.9	61.2	69.7	77.3
$\Lambda$	30.0	36.3	42.1	47.3
$\bar{\Lambda}$	29.2	35.4	41.1	46.2
$\Xi^-$	4.45	5.47	6.41	7.23
$\Xi^+$	4.36	5.38	6.31	7.14
$\Omega^-$	0.772	1.038	1.314	1.586
$(B - \bar{B})^{**}$	4.81	5.60	6.29	6.88
$\rho$	92.4	96.6	99.1	100.3
$\phi$	19.0	20.5	21.4	21.9
$K^{0*}(892)$	42.6	45.3	46.9	47.6
$K^{0*}(892)/K^-$	0.301	0.322	0.337	0.348
$\phi/K^{0*}(892)$	0.446	0.452	0.456	0.460
$\pi^0$	942	933	925	916
$\eta$	110	111	111	110
$\eta'$	9.67	10.4	10.8	11.1
$\pi_{WD}^0$	1251	1251	1249	1245

Yield of strangeness is slightly increasing, this increase is in heavy mass strange baryons, e.g.,  $\Lambda$ , and this depletes slightly the yield of kaons. Overall the specific strangeness per entropy yield grows very slowly from  $s/S = 0.0245$  to 0.027. Several ratios, such as  $\phi/K^{0*}(892) \simeq 0.45$ , where several effects compensate are nearly constant.

We also show the post-weak decay  $\pi_{WD}^0$  yield which is relatively large and independent of hadronization  $T$ . The decay  $\pi^0 \rightarrow \gamma\gamma$  generates a strong electromagnetic energy component.

**LHC prediction within non-equilibrium SHM:** Within the non-equilibrium hadronization approach, we need to further anchor the two quark pair abundance parameters  $\gamma_q$  and  $\gamma_s$ . In absence of experimental data, we introduce additional hadronization conditions, the relative strangeness yield  $s/S$  and hadronization pressure  $P$ . We vary  $P$ , see table II, just as we varied  $T$  the hadroniza-

TABLE II: Chemical non-equilibrium particle yields, each column for different hadronization pressure. See caption of table I for further details.

$P^*$ [MeV/fm <sup>3</sup> ]	60.3	70.0	82.2	90.1
$(s/S)^*$	0.0367	0.0370	0.0370	0.0373
$\lambda_q^*$	1.0055	1.0055	1.0055	1.0055
$10^3(\lambda_s - 1)^{**}$	2.69	2.45	2.19	2.04
$(Q/B)^*$	0.400	0.400	0.4000	0.4000
$(s - \bar{s})^*$	0.0000	0.0000	0.0000	0.0000
$(dh/dy)^*$	1800	1800	1800	1800
$T$ [MeV]	131.2	134.3 ± 0.1	137.7 ± 0.1	139.6 ± 0.1
$\gamma_q$	1.599 ±0.001	1.600 ±0.008	1.601 ±0.009	1.599 ±0.011
$\gamma_s$	2.913 ±0.008	2.842 ±0.030	2.745 ±0.030	2.721 ±0.016
$dV/dy$ [fm <sup>3</sup> ]	5469±542	4731±136	4043±119	3705±168
$dS/dy$	13924	13879	13794	13797
$E/Ts$	1.060	1.060	1.059	1.059
$P/E$	0.170	0.168	0.165	0.164
$E/V$ [GeV/fm <sup>3</sup> ]	0.354	0.417	0.497	0.550
$\pi^-, \pi^+$	858	854	850	848
$K^-$	192.0	190.2	186.5	186.2
$K^+$	192.9	191.2	187.5	187.3
$p$	32.9	36.3	40.3	42.5
$\bar{p}$	31.8	35.2	39.0	41.2
$\Lambda$	28.9	31.8	34.8	36.9
$\bar{\Lambda}$	28.1	31.0	33.9	35.9
$\Xi^-$	6.92	7.56	8.12	8.60
$\Xi^+$	6.77	7.40	7.96	8.43
$\Omega^-$	1.56	1.73	1.89	2.03
$(B - \bar{B})^{**}$	3.640	3.973	4.328	4.539
$\rho$	56.1	58.8	61.7	63.2
$\phi$	30.0	30.7	30.8	31.4
$K^{0*}(892)$	39.9	41.4	42.6	43.6
$K^{0*}(892)/K^-$	0.208	0.218	0.228	0.234
$\phi/K^{0*}(892)$	0.751	0.741	0.722	0.721
$\pi^0$	988	983	979	977
$\eta$	134	132	128	128
$\eta'$	10.4	10.7	10.8	11.0
$\pi_{WD}^0$	1398	1396	1389	1391

tion condition in the chemical equilibrium model. In the chemical non-equilibrium SHM, two conditions suffice to narrow considerably the values of three SHM parameters ( $\gamma_q$ ,  $\gamma_s$  and  $T$ ), but only if we insist that a third condition  $E/Ts > 1$  is qualitatively satisfied.

Strangeness yield is a natural hadronization condition of QGP. We consider the ratio of strangeness per entropy  $s/S$  in which  $T^3$  coefficients and other systematic dependencies cancel. Since the entropy contents is directly related to the particle multiplicity  $dh/dy$ , in our case  $s/S$  implies  $s$ -yield and directly relates to strangeness pair yield. In QGP,  $s\bar{s}$ -pairs are produced predominantly in thermal gluon processes and their yield can be obtained within the QCD perturbative approach. In a study which was refined to agree with the strangeness yield observed at RHIC, we predicted the value  $s/S \simeq 0.037$  for LHC [16]. We use here this result, noting that higher  $s/S$  values are possible, depending on LHC formed QGP dynamics. The QGP expected dynamic strangeness yield is considerably higher than the chemical equilibrium yield, table I,  $0.0270 \leq s_{eq}/S \leq 0.0245$ . The greater

strangeness content in QGP is, in fact, the reason behind the interest in strangeness as signature of QGP.

The second condition arises from the observation that once the statistical parameters were fitted across diverse reaction conditions at RHIC, the one constant outcome was that the hadronization pressure  $P = 82$  MeV/fm<sup>3</sup> [17]. Choice of pressure as a natural QGP hadronization constraint is further rooted in the observation that the vacuum confinement phenomenon can be described within the qualitative MIT-bag model of hadrons introducing vacuum pressure is  $B_{\text{MIT}} = 58$  MeV/fm<sup>3</sup>, while in a bag-motivated fit to hadron spectra which allows additional flexibility in parameters one finds  $B_{\text{fit}} = 112$  MeV/fm<sup>3</sup> [18]. Clearly, a range of values is possible theoretically, with the hadronization condition  $P = 82$  MeV/fm<sup>3</sup> right in the middle of this domain. We will use this ‘critical pressure’ hadronization condition as our constraint, but also vary it such that  $60 \leq P \leq 90$  MeV/fm<sup>3</sup> so that we can be sure that our prediction is not critically dependent on the empirical value. The pressure seen in equilibrium model case, table I, has a range  $64 \leq P \leq 230$  MeV/fm<sup>3</sup>.

The third constraint is not imposed in its precise value, but we require that hadronization occurs under the constraint that  $E/TS > 1$ . In comparison, for the equilibrium case, table I, we have  $0.86 < E/TS < 0.87$  a relatively small variation. The importance of this quantity  $E/TS > 1$  as a diagnostic tool for explosive QGP outflow and hadronization was discussed in [14]. In fact, we find that a reasonable and stable hadronization arises in chemical non-equilibrium within a narrow interval  $1.059 < E/TS < 1.060$ .

In table II, the outcome of this procedure is presented. We state the actual values of parameters for which solution of all constraints was numerically obtained, thus in first column pressure is not 60 but 60.3 MeV/fm<sup>3</sup>. With rising hadronization pressure, the hadronization temperature rises, but it remains well below the phase transformation temperature. As we have discussed, the low value of  $T$  in the chemical non-equilibrium SHM is consistent with the dynamics of the expansion, the flow of matter reduces the phase balance  $T$ . This in turn is then requiring that the light quark abundance parameter  $\gamma_q \simeq 1.6$ . This is the key distinction of the chemical non-equilibrium. It further signals enhancement of production of baryons over mesons by just this factor. Note that  $\gamma_s/\gamma_q \simeq 1.72$ . This large ratio means that the yield of  $\Lambda$  and  $p$  do not differ much. This indicates strong enhancement of strangeness, a first day observable of QGP formation, along with  $\phi$  enhancement [19].

**Comparison of SHM results:** The large bulk hadronization volume  $dV/dy \simeq 4500$  fm<sup>3</sup> is suggesting that there will be noticeable changes in the HBT observables allowing to produce such a great hadronization volume. The bulk energy content is found in both approaches to be  $dE/dy = E/V \times dV/dy = 2.00 \pm 0.05$  TeV per unit of rapidity at  $y = 0$ . This is the thermal energy of QGP prior to hadronization measured in the

local fluid element rest frame.

The entropy content in the bulk for non-equilibrium,  $dS/dy = 13860 \pm 64$ , is 5% smaller compared to equilibrium case. This is due to the fact that non-equilibrium particle yields do not maximize entropy. We note that the yields of pions, kaons, and even single strange hyperons are remarkably independent of hadronization pressure, or, in the equilibrium case, temperature, even though the volume parameter changes greatly. This effect is counteracted by a balancing change in hadronization temperature since the yield of charged hadrons is fixed. The hadronization energy density is very close to  $E/V \simeq 0.5$  GeV/fm<sup>3</sup>, and it tracks the pressure since the ratio  $P/E$  is found to be rather constant.

The yield of multistrange hadrons is much enhanced in chemical non-equilibrium model, compared to the equilibrium model, on account of 50% increased yield of strangeness, which is potentiated for multistrange particles as was predicted to be the signature of QGP [19]. The yield of  $\Lambda$ , for the most favored hadronization condition in both equilibrium and non-equilibrium, can in fact be lower in the non-equilibrium case than in the equilibrium, yet at LHC the yield of  $K$  is always 40% greater. Like in the equilibrium results, we observe that several yields are largely independent of the hadronization condition, meaning that ratios such as  $\phi/h$  could be a distinctive signature of hadronization, differentiating the two primary models. This is illustrated in figure 1 where the ratio is shown as function of resultant hadronization  $T$ .

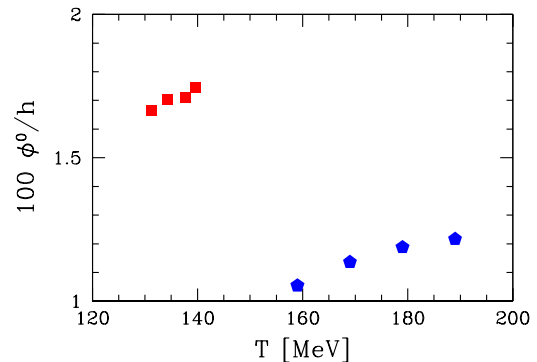


FIG. 1: (color on-line) Specific yield  $\phi/h$  for chemical equilibrium model to right bottom (blue) and chemical non-equilibrium model left up (red).

One can, however, argue that  $\phi/h$ , seen in Fig. 1, could be brought about by strangeness enhancement, not requiring that  $\gamma_q > 1$ , for a more complete discussion see [20]. To narrow the choices, we propose to study two more ratios, shown in Fig. 2. The top section shows  $K^*/K^-$ , as function of the yield  $K^-/h$ . The lower right (red) non-equilibrium result shows strangeness enhancement at low hadronization  $T$  since  $K^*/K^-$  mainly depends on  $T$ . We have shown both particle and antiparticle ratios derived from our fixed input for net baryon yield to illustrate that differentiation of these results will not be easily possible.

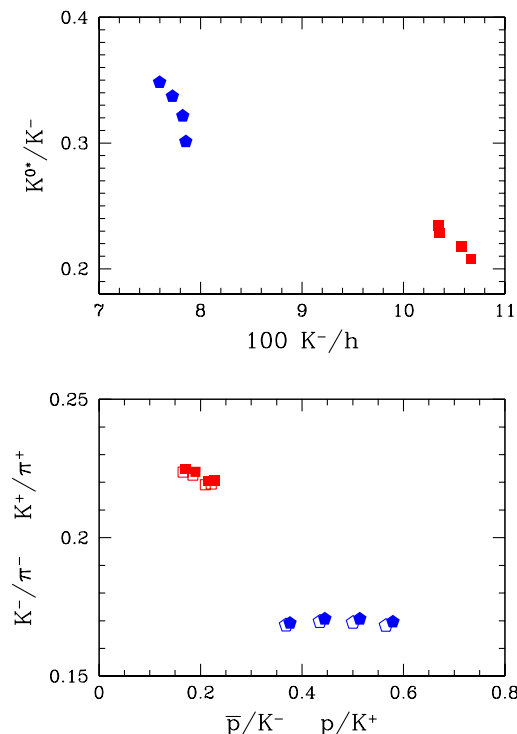


FIG. 2: (color on-line) Top: ratio of resonance  $K^*$  to kaon yield  $K$ , as function of specific kaon yield  $K^-/h$ , the equilibrium model (blue) is left up and chemical non-equilibrium (red) is bottom right. Bottom frame: the  $K/\pi$  ratio as function of  $p/K$  ratio. Bottom right (blue) is equilibrium model and upper left is non-equilibrium model.

The bottom section, in Fig. 2, shows the strangeness enhancement in format of  $K/\pi$  as function of the easiest to measure baryon to meson ratio which is a measure of

absolute magnitude of  $\gamma$ , here specifically,  $\gamma_q^3/\gamma_s\gamma_q$ . We see the equilibrium model to lower right (blue) while the non-equilibrium model is upper left.

**Summary and conclusions:** We have obtained particle yields within the statistical hadronization model for the LHC-ion run at  $\sqrt{s_{NN}} = 2.76$  TeV. We have discussed both bulk properties of QGP at breakup and the resulting particle yields. These can vary significantly depending on the hadronization mechanism. Distinctive features associated with QGP based strangeness enhancement and final state chemical non-equilibrium were described and strategies leading to better understanding of chemical (non-)equilibrium were proposed.

We have shown how enhanced yield of strangeness with the phase space occupancy  $\gamma_s \simeq 2.75$  when  $\gamma_q \simeq 1.6$  modifies the yield of strange hadrons and detailed predictions for the observables such as  $\phi/h$ ,  $K^*/K$ ,  $K/\pi$ ,  $p/K$ ,  $\Lambda/p$  were offered. Enhanced yields of (multi)strange particles are tabulated. We note that absolute yield of  $\phi$  is enhanced by a factor 1.5 in the non-equilibrium compared to equilibrium hadronization. There is no significant dependence of the  $\phi$  yield on hadronization condition making it an ideal first day differentiating chemical equilibrium from non-equilibrium.

The large bulk hadronization volume  $dV/dy \simeq 4500 \text{ fm}^3$  related to HBT observables, the local rest frame thermal energy content  $dE/dy|_0 = 2$  TeV constrains hydrodynamic models. A large yield of  $\pi^0$ ,  $\eta$  and thus of associated decay photons is noted, enhanced somewhat in the chemical non-equilibrium case.

**Acknowledgments** LPTHE: Laboratoire de Physique Théorique et Hautes Energies, at University Paris 6 and 7 is supported by CNRS as Unité Mixte de Recherche, UMR7589. This work was supported by a grant from the U.S. Department of Energy, DE-FG02-04ER41318

- 
- [1] S. Borsanyi *et al.*, JHEP **11**, 077 (2010). DOI: 10.1007/JHEP11(2010)077 see also: arXiv:1011.4230 [hep-lat], arXiv:1011.4229 [hep-lat].
  - [2] K. Aamodt *et al.* [The ALICE Collaboration], arXiv:1011.3916 [nucl-ex].
  - [3] P. Bozek, M. Chojnacki, W. Florkowski and B. Tomasik, Phys. Lett. B **694**, 238 (2010)
  - [4] G. Torrieri *et al.*, Comput. Phys. Commun. **167**, 229 (2005); Comput. Phys. Commun. **175**, 635 (2006)
  - [5] J. Letessier and J. Rafelski, Eur. Phys. J. A **35**, 221 (2008)
  - [6] A. Andronic, P. Braun-Munzinger and J. Stachel, Nucl. Phys. A **772**, 167 (2006)
  - [7] A. Andronic, P. Braun-Munzinger and J. Stachel, Phys. Lett. B **673**, 142 (2009)
  - [8] F. Becattini, P. Castorina, A. Milov and H. Satz, Eur. Phys. J. C **66**, 377 (2010)
  - [9] J. Rafelski, J. Letessier and G. Torrieri, Phys. Rev. C **72**, 024905 (2005)
  - [10] A. Andronic *et al.*, Nucl. Phys. A **837**, 65 (2010)
  - [11] P. de Forcrand, PoS **LAT2009**, 010 (2009) [arXiv:1005.0539 [hep-lat]].
  - [12] G. Endrodi, Z. Fodor, S. D. Katz and K. K. Szabo, PoS **LAT2008**, 205 (2008) [arXiv:0901.3018 [hep-lat]]. Z. Fodor and S. D. Katz, arXiv:0908.3341 [hep-ph].
  - [13] J. Cleymans, J. Phys. G **37** (2010) 094015.
  - [14] J. Rafelski and J. Letessier, Phys. Rev. Lett. **85**, 4695 (2000)
  - [15] J. Rafelski and J. Letessier, J. Phys. G **35**, 044042 (2008), and Eur. Phys. J. C **45**, 61 (2006).
  - [16] J. Letessier and J. Rafelski, Phys. Rev. C **75**, 014905 (2007)
  - [17] J. Rafelski and J. Letessier, J. Phys. G **36**, 064017 (2009)
  - [18] A. T. M. Aerts and J. Rafelski, Phys. Lett. B **148**, 337 (1984).
  - [19] J. Rafelski, Phys. Rept. **88**, 331 (1982).
  - [20] M. Petran and J. Rafelski, Phys. Rev. C **82**, 011901 (2010) M. Petran, J. Letessier, V. Petracek and J. Rafelski, arXiv:1010.3749 [hep-ph].